

Laser Scheme for Doppler Cooling of the Hydroxyl Cation (OH⁺)

Published as part of *The Journal of Physical Chemistry virtual special issue "Physical Chemistry of Quantum Information Science"*.

Niccolò Bigagli, Daniel W. Savin, and Sebastian Will*



Cite This: *J. Phys. Chem. A* 2023, 127, 8194–8199



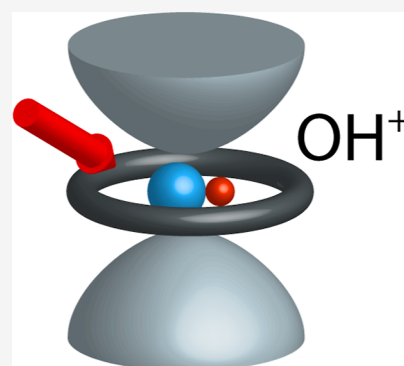
Read Online

ACCESS |

Metrics & More

Article Recommendations

ABSTRACT: We report on a cycling scheme for Doppler cooling of trapped OH⁺ ions using transitions between the electronic ground state X³Σ⁻ and the first excited triplet state A³Π. We have identified relevant transitions for photon cycling and repumping, have found that coupling into other electronic states is strongly suppressed, and have calculated the number of photon scatterings required to cool OH⁺ to a temperature where Raman sideband cooling can take over. In contrast to the standard approach, where molecular ions are sympathetically cooled, our scheme does not require co-trapping of another species and opens the door to the creation of pure samples of cold molecular ions with potential applications in quantum information, quantum chemistry, and astrochemistry. The laser cooling scheme identified for OH⁺ is efficient despite the absence of near-diagonal Franck–Condon factors, suggesting that broader classes of molecules and molecular ions are amenable to laser cooling than commonly assumed.



INTRODUCTION

Laser cooling and quantum control of atoms and atomic ions has enabled a plethora of scientific investigations over the last few decades.^{1–4} In recent years, the field has expanded toward molecules^{5–9} as their more complex quantum state structure opens a broader scope of physics to be studied, including measurements of fundamental constants,^{10–12} investigations of quantum chemistry,^{13–15} applications in quantum information,^{6,7,16} and access to novel many-body quantum systems.¹⁷ Identifying molecules that are relevant for scientific and technological applications and at the same time amenable to laser cooling is an active area of research, but, so far, it has almost exclusively focused on neutral molecules.^{18–23}

Molecular ions have broad scientific use cases.⁶ Progress on laser cooling and quantum control schemes for molecular ions promises to open new scientific avenues, building on the enormous success of atomic ions in quantum science.^{1,24} For quantum information, the rich internal structure of molecular ions may allow the realization of efficient gate operations and long qubit storage times^{16,25} in the same physical system, akin to neutral molecules.^{26–28} Molecular ions enable Coulomb-mediated two-qubit operations²⁹ and have been proposed as an alternative to neutral molecules.^{30,31} They also may allow the realization of qudits, multi-level systems that constitute a powerful extension of the qubit-based quantum information paradigm.^{32,33} In addition, cold molecular ions in well-defined quantum states can be employed in collisional studies in quantum chemistry and astrochemistry. For example, gas-phase chemistry in cold interstellar clouds is driven by ion-neutral

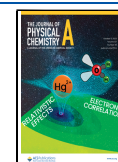
reactions where the ions are in their lowest electronic, vibrational, and rotational levels due to the relaxation of internal excitations close to the 2.7 K cosmic microwave background.^{34,35} Fully quantum mechanical calculations for these reactions are beyond current computational capabilities for systems with four or more atoms. Therefore, laboratory measurements with molecules in quantum states similar to those in interstellar space would be helpful to elucidate the chemical kinetics.^{36–40}

Today, the standard approach to the preparation of trapped molecular ions relies on sympathetic cooling via a co-trapped ionic^{28,41} or neutral⁴² atomic species. Direct laser cooling of molecular ions has not been explored extensively. Although cooling via co-trapped species has proven effective and useful,³¹ it is technically challenging. In addition, for sensitive applications in quantum information and precision measurements, where high fidelity and low dephasing are critical,⁴³ the presence of a second species may eventually be limiting.^{30,44} All-optical cooling schemes should be highly attractive, but, so far, only a few theoretical studies on the prospects of laser cooling of molecular ions exist,⁴⁴ and most have not accounted

Received: May 16, 2023

Revised: July 27, 2023

Published: September 22, 2023



for the full rovibrational structure of the ion under investigation.^{45–47}

In this article, we discuss a laser-cooling scheme for the hydroxyl cation, OH⁺. We envision the scheme to be applied to a single ion or an ensemble of ions held in a deep and tightly confining ion trap, as schematically illustrated in Figure 1a. In

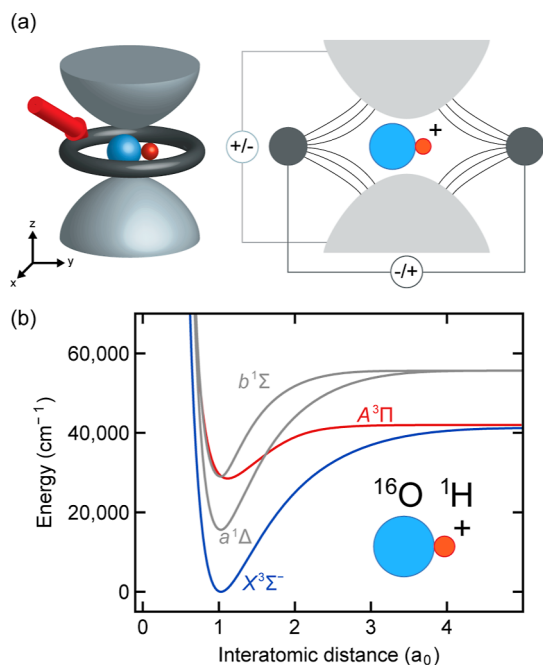


Figure 1. Laser cooling of OH⁺ ions trapped in an ion trap. (a) Schematic of an OH⁺ ion in a cylindrical quadrupole ion trap.⁵⁷ The left image shows a three-dimensional sketch of the ion trap; the right image shows a cross-section, including field lines. The specific trap shown is for illustration purposes only; the cooling scheme is general and can be implemented in other types of ion traps. The cooling and repumping beams are incident collinearly from one direction that has a finite angle with all three Cartesian axes of the trap, providing cooling in three dimensions. (b) Potential energy curves of OH⁺.⁵² Depicted are the low-lying electronic potentials relevant to this study, two with triplet spin character and two with singlet spin character. The inset shows a pictorial representation of an OH⁺ molecular ion.

this setting, three-dimensional laser cooling can be achieved with cooling and repumping laser beams incident from a single direction that has a finite angle with all three Cartesian axes of the trap.⁴⁸ The proposed scheme can provide cooling in the Doppler regime, where the motional energy of the ion is significantly larger than the trap frequency.³¹ To cool below the Doppler limit, a secondary Raman sideband cooling step may be employed.⁴⁴ However, in this work, we solely focus on the description of the Doppler cooling scheme for OH⁺.

The OH⁺ ion is particularly relevant in the context of astrophysics and astrochemistry. The production of cold, pure, and trapped samples of OH⁺ would enable reaction studies that can help shed light on processes such as the cosmic ray ionization rate of the interstellar medium⁴⁹ and the gas-phase pathway to the formation of water.⁵⁰ Additional uses of laser-cooled OH⁺ molecules may be in quantum information. Due to large rotational spacings ($B \sim 500$ GHz⁵¹), coherent control of rotational qubits in OH⁺ would be challenging but possible via a two-photon Raman transfer. Given that Doppler cooling schemes have not been widely discussed for molecular ions, this study also uses OH⁺ as a proof-of-concept case that may

encourage the development of laser cooling schemes for other molecular ions.

The relevant low-lying potential energy curves of OH⁺ are shown in Figure 1b.⁵² OH⁺ has favorable characteristics for laser cooling. Its energy level structure is relatively simple, with its first few electronic states having either a triplet or a singlet nature. Furthermore, OH⁺ is extremely tightly bound. As can be seen from the minima of the potential energy curves (see Figure 1b), the bond length is about one a_0 , where a_0 is the Bohr radius. As a result, the vibrational and rotational energy spacings are large, of the order of 3000 and 60 cm⁻¹, respectively. Due to the large vibrational spacing, only about a dozen vibrational states exist in the X³Σ⁻ potential below the A³Π potential, which limits the number of decay channels for potential transitions of a laser cooling scheme. However, there is no transition in OH⁺ with a near-diagonal Franck–Condon factor (FCF), a characteristic that is often believed necessary for a functional cooling scheme.⁴⁴ The highest branching ratio for a single transition is 0.56.⁵³ Despite this complication, as we demonstrate below, OH⁺ supports a laser cooling scheme that is not more complex than state-of-the-art cooling schemes for neutral molecules.⁵⁴ OH⁺ also has a non-zero nuclear spin of $I = 1/2$,⁵⁵ which we do not explicitly take into account in this study. However, we do not expect the resulting hyperfine structure to fundamentally prevent the laser cooling from functioning, as has been seen in earlier demonstrations of laser cooling.⁵⁶

■ LASER CYCLING SCHEME

The proposed cycling scheme makes use of transitions between the electronic ground state of the molecule, X³Σ⁻, and its first electronically excited triplet state, A³Π. The specific transitions of the scheme are shown in Figure 2. We explain below how a sufficient degree of closure can be reached. The required spectroscopic data were extracted from the ExoMol database,⁵⁸ which for OH⁺ relies on the optical transitions published in

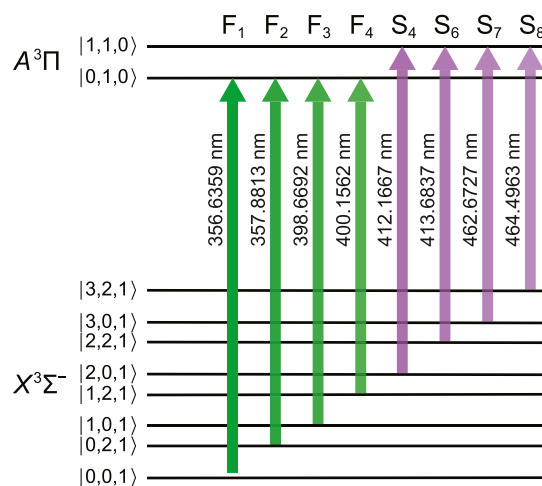


Figure 2. Laser cooling scheme. The green (purple) arrows represent the cooling and repumping beams from the X³Σ⁻ ground electronic state to the A³Π |0, 1, 0⟩ (|1, 1, 0⟩) state. The numbers on the left represent the quantum numbers $|v, N, J\rangle$. To the left of each arrow, we indicate the wavelength of each transition. Transitions from left to right are ordered from smaller to larger transition wavelength and larger to smaller transition strength. The labels above each transition for the first (F) and second (S) legs of the cooling scheme are introduced for easier comparison to Figure 3.

refs 51 and 59. We utilize the provided energy levels, transition frequencies, and Einstein A coefficients.

The logic of the cooling scheme is as follows: we start from the absolute molecular ground state, $X^3\Sigma^- \nu = 0, N = 0, J = 1$), following Hund's case (b),⁶⁰ where ν , N , and J are the vibrational quantum number, the angular momentum excluding the electron and nuclear spins, and the angular momentum excluding the nuclear spin, respectively. Due to the $\Delta J = \pm 1$ selection rule, excitation to both $J = 0$ and $J = 2$ states is possible. Excitation to $J = 0$ is favorable as the only decay channel is to $J = 1$, reducing the number of needed repumper lasers by a factor of two. In addition, excitation to a low-lying vibrational state is favorable due to higher FCFs. Thus, we choose $A^3\Pi |0, 1, 0\rangle$ as the first excited state of the scheme. The main decays of this state are to the eight $X^3\Sigma^-$ states shown in Figure 2, with only two other observed decays with negligible branching ratios ($\sim 10^{-8}$). Overall, the scattering rate of $A^3\Pi |0, 1, 0\rangle$ is relatively small at $3.5 \times 10^5 \text{ s}^{-1}$ and by itself would lead to long cooling times. By adding a second excited state to the cycling scheme, the $A^3\Pi |1, 1, 0\rangle$ state, it is possible to speed up the cooling time by about a factor of two, as is discussed below.

The excited $A^3\Pi |0, 1, 0\rangle$ and $A^3\Pi |1, 1, 0\rangle$ states have 6 and 8 decay channels, respectively, with branching ratios above 10^{-3} , as shown in Figure 3. This is a practical threshold for the

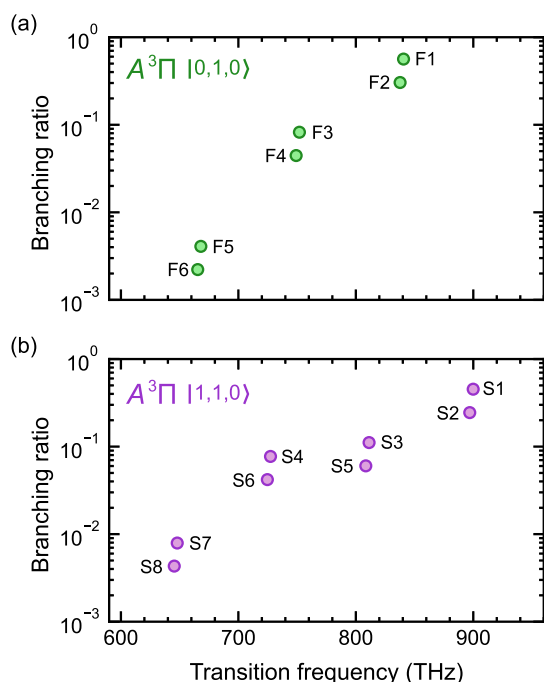


Figure 3. Branching ratios for decay from the excited states considered here (a) $A^3\Pi |0, 1, 0\rangle$ and (b) $A^3\Pi |1, 1, 0\rangle$. The decay paths for each scheme are numbered in the order of decreasing branching ratios and the labels and color coding refer to the transitions shown in Figure 2. All decays are to the same states in the $X^3\Sigma^-$ manifold illustrated in Figure 2.

relevance of a transition in a typical laser cooling scheme.⁶¹ Branching ratios are calculated using the Einstein coefficients A_i for spontaneous decay to state i ⁵⁸ through the relation $BR_i = A_i / \sum_j A_j$, where the sum runs over all possible radiative decay paths to a lower energy state j for a given $A^3\Pi$ state.

We have investigated the question whether the loss to other states could potentially hamper the $X^3\Sigma^- \leftrightarrow A^3\Pi$ cooling

scheme. We find that the effects of state mixing between $A^3\Pi$ and the singlet states $b^1\Sigma^+$ and $a^1\Delta$ should be minimal. For the nearby $b^1\Sigma^+$ state, spin-orbit coupling with a strength of about 75 cm^{-1} ⁶² leads to an admixture of 0.5% $b^1\Sigma^+ |\nu = 0\rangle$ to the $A^3\Pi |\nu = 0, 1\rangle$ states, calculated from the diagonalization of the Hamiltonian of these states with an off-diagonal spin-orbit contribution. Although this is a non-negligible admixture, it is not expected to lead to relevant losses out of the cycling scheme (see the Appendix). This is due to the unusual structure of OH^+ , where decay from $b^1\Sigma^+$ to $a^1\Delta$ is suppressed by the $\Delta\Lambda = 0, \pm 1$ selection rules.⁶³ Furthermore, direct coupling between $b^1\Sigma^+$ and vibrationally excited $a^1\Delta$ states should not be an issue as the only loss channel via mixing of $a^1\Delta$ can be due to relaxation into lower vibrational states of $a^1\Delta$. However, spontaneous decay between vibrational states is suppressed in the first order⁶³ and driving of such transitions by black-body radiation would be slow compared to the timescale of the cooling scheme. In line with these arguments, to our knowledge, such decays in OH^+ have not been reported. Finally, we note that the loss from predissociation⁶⁴ is fully suppressed for the $X^3\Sigma^- \leftrightarrow A^3\Pi$ cooling scheme.

RESULTS AND DISCUSSION

Using the branching ratios from Figure 3, we quantify the closure that can be achieved by adding an increasing number of repumping transitions. We calculate the number of scatterings that will lead to a probability of 10% ($n_{10\%}$) and of 90% ($n_{90\%}$) for retaining an ion in the cycling scheme.⁶⁵ Calculations are made assuming the use of two excited states, as shown in Figure 2. We employ a Monte Carlo model in which an ion is initialized in the ground state and then each scattering event is simulated by updating the probability of populating each state in the cooling scheme after each step. Table 1 shows the results of these calculations. The quantity p is the closure of the scheme, calculated via $n_{x\%} = \ln(x/100)/\ln(p)$.⁶⁵ A conservative estimate of the time to complete $n_{x\%}$ scattering events, $t_{x\%}$ is also provided. To calculate this quantity, we use the relation $t_{x\%} = n_{x\%}/R$, where $R = \Gamma / (G + 1 + 2 \sum I_{\text{sat},i} / I_i)$ is the scattering rate.^{66,67} Here, Γ is the excited state linewidth, G is the number of driven transitions, $I_{\text{sat},i} = \pi h c \Gamma / 3 \lambda_i^3$ is the saturation intensity⁶⁷ of the i th transition, and I_i is the intensity of the laser addressing said transition, set to $I_i = 10^3 \text{ mW cm}^{-2}$, which is an intensity that is easily achievable in an experiment at the given wavelengths. In the definition of the saturation intensity, c is the speed of light and λ_i is the wavelength of the addressed transition. Our calculation of R results in an overestimate of $t_{x\%}$ as the expression for R assumes a single excited state, only $A^3\Pi |0, 1, 0\rangle$. In an experiment, where several repumping transitions cycle through a second excited state, here, $A^3\Pi |1, 1, 0\rangle$, the scattering rate is boosted and the cooling time is lowered, as has been experimentally demonstrated in laser cooling schemes for neutral molecules, e.g., in ref 22.

We calculate the number of scatterings, n_{cool} , required to bring the sample to close-to-zero motional temperature from room (300 K) and cryogenic (4 K) temperatures. In addition, we calculate the time t_{cool} necessary for this process. For the experimental setup, we assume that the ion is electrostatically trapped and that cooling and repumping laser beams come from a single direction that has a finite angle with all three Cartesian trap axes, as illustrated in Figure 1a. Using a single incoming direction for the lasers enables cooling in all spatial directions, thanks to the confinement provided by the ion trap,

Table 1. Closure, Number of Scatterings, and Scattering Time for an Increasing Number of Repumping Transitions

driven transitions	p	$n_{10\%}$	$t_{10\%}$ (ms)	$n_{90\%}$	$t_{90\%}$ (ms)
F1	0.631	5	0.02	1	
F1–F2	0.873	17	0.1	1	
F1–F3	0.950	45	0.5	3	0.02
F1–F4	0.994	361	5	17	0.2
F1–F4, S4	0.997	918	17	43	0.8
F1–F4, S4, S6	0.9986	15,941	800	731	36
F1–F4, S4, S6–S7	0.99995	44,287	2.6×10^3	2028	100
F1–F4, S4, S6–S8	0.9999997	2,563,381	1.9×10^6	117,295	9.0×10^4

as suggested in ref 48, and greatly simplifies the laser setup. Table 2 summarizes the results. Cooling OH⁺ ions down from

Table 2. Results of the Photon Scatterings Analysis Starting at Cryogenic Temperature and Room Temperature

$T = 4$ K		$T = 300$ K	
n_{cool}	t_{cool} (ms)	n_{cool}	t_{cool} (ms)
2.3×10^3	45	2.0×10^4	400

room temperature will require 2×10^4 scattering events. Comparing this requirement to the results in Table 1, this can be achieved with 90% efficiency within <500 ms using 8 transitions (F1–F4, S4, and S6–S8) (Note that S5 represents a decay to state $X^3\Sigma^- |1, 2, 1\rangle$ which is already repumped by F4, such that no additional repumper on S5 is necessary.). Cooling OH⁺ ions from cryogenic temperatures will require 2.3×10^3 scattering events, which can be achieved with 90% efficiency within <500 ms using 6 transitions (F1–F4, S4, and S6). We note that OH⁺ can be easily produced at cryogenic temperatures, as demonstrated in an earlier work via electronic impact on water vapor.^{38,40} It is important to note that in practical experiments, less stringent requirements on the probability of retention should be acceptable. For a 10% probability of retention, cooling from room temperature can be achieved with 6 to 7 lasers (F1–F4, S4, and S6–S7) within about 1 s and from cryogenic temperatures with 5 to 6 lasers (F1–F4, S4, and S6) within about 50 ms. Hence, on average, it would take 10 s and 0.5 s, respectively, to successfully initialize the system, a time that is short compared to the storage time of a molecular ion once it is trapped and cooled.

CONCLUSIONS

In summary, we have presented a direct laser cooling scheme of OH⁺. The scheme is expected to work both for a single trapped ion and for trapped ensembles. In the case of an ensemble, the direction of the laser cooling beams could even be arbitrary as the Coulomb interactions in the ensemble are expected to couple all directions of motion.³¹ While the scheme requires some technical effort, laser cooling of OH⁺ would come with several benefits: cold samples can be prepared without the need for sympathetic cooling via neutral or ionic atoms, and temperatures can be efficiently reached where Raman sideband cooling can take over to cool ions to the vibrational ground state (of the trap). Rapid progress in laser technology⁶⁸ promises to drastically reduce the technical complications involved in a cooling scheme with multiple lasers. Also, due to the confined trapping region of an ion trap, the lasers can be tightly focused, and we expect that only very moderate laser powers will be necessary. Once cooled, OH⁺ will enable studies relevant for gas-phase astrochemistry of

interstellar clouds. Furthermore, quantum control of OH⁺ will be an enabling step for its use as a qubit or a qudit in quantum information experiments. Finally, this work, similar to the case of C₂ that we discussed in an earlier work,⁶¹ suggests that molecules with non-diagonal FCFs can also be amenable to laser cooling. We hope that this work will inspire further investigations on the application of laser cooling techniques to more complex molecules that are scientifically relevant but have so far been deemed unsuitable for laser cooling.

APPENDIX

As noted in the main text, a loss channel for the $X^3\Sigma^- \leftrightarrow A^3\Pi$ cooling scheme could arise from spin–orbit coupling between $A^3\Pi$ and nearby singlet states. Here, we provide more detail to show that such processes should be sufficiently suppressed for practical purposes. As mentioned in the main text, the 0.5% admixture of $b^1\Sigma^+$ ($\nu = 0$) to the $A^3\Pi$ ($\nu = 0, 1$) states does not open up a loss channel to the first order due to prohibitive selection rules. To second order, decay could happen via the admixture of $^1\Pi$ character to the $b^1\Sigma$ potential, with the closest $^1\Pi$ state lying about 15,000 cm⁻¹ above the $b^1\Sigma$ potential.⁵² With a coupling constant of 75 cm⁻¹ (assuming a coupling similar to $b^1\Sigma^+$ and $A^3\Pi$; to our knowledge, there is no reported literature value), this leads to a 10^{-5} admixture of $^1\Pi$ character to the $b^1\Sigma$ state. Taken together, this amounts to a loss channel on the 5×10^{-8} level. Loss channels allowed through higher order processes should contribute significantly less. Also, direct coupling between $A^3\Pi$ and $a^1\Delta$ is not expected to lead to significant loss. The only decay path out of the cycling scheme would be spontaneous decay into lower lying vibrational states of $a^1\Delta$, which is forbidden.⁶³ Based on these arguments, it is highly probable that the proposed cooling scheme will be sufficiently closed, especially taking into account that only closure to the 10^{-4} level will be needed for the scheme to be practically useful (see the main text and Table 2).

AUTHOR INFORMATION

Corresponding Author

Sebastian Will – Department of Physics, Columbia University, New York, New York 10027, United States; orcid.org/0000-0003-2672-5264; Email: sebastian.will@columbia.edu

Authors

Niccolò Bigagli – Department of Physics, Columbia University, New York, New York 10027, United States

Daniel W. Savin – Columbia Astrophysics Laboratory, Columbia University, New York, New York 10027, United States

Complete contact information is available at:

<https://pubs.acs.org/10.1021/acs.jpca.3c03248>

Notes

The authors declare no competing financial interest.

ACKNOWLEDGMENTS

We thank Peter F. Bernath, Tim de Jongh, Ábel Kálosi, Ian Stevenson, and Sergey Yurchenko for stimulating discussions and Octavio Roncero for help with the potential energy curves. This work was supported by a Columbia University Research Initiative in Science and Engineering (RISE) award. D.W.S. was additionally supported by the NASA Astrophysics Research and Analysis program under 80NSSC19K0969. S.W. acknowledges additional support from the Alfred P. Sloan Foundation.

REFERENCES

- (1) Leibfried, D.; Blatt, R.; Monroe, C.; Wineland, D. Quantum dynamics of single trapped ions. *Rev. Mod. Phys.* **2003**, *75*, 281–324.
- (2) Bloch, I.; Dalibard, J.; Zwirger, W. Many-body physics with ultracold gases. *Rev. Mod. Phys.* **2008**, *80*, 885–964.
- (3) Buluta, I.; Nori, F. Quantum simulators. *Science* **2009**, *326*, 108–111.
- (4) Blatt, R.; Roos, C. F. Quantum simulations with trapped ions. *Nat. Phys.* **2012**, *8*, 277–284.
- (5) Ni, K.-K.; Ospelkaus, S.; De Miranda, M.; Pe’Er, A.; Neyenhuis, B.; Zirbel, J.; Kotochigova, S.; Julienne, P.; Jin, D.; Ye, J. A high phase-space-density gas of polar molecules. *Science* **2008**, *322*, 231–235.
- (6) Carr, L. D.; DeMille, D.; Krens, R. V.; Ye, J. Cold and ultracold molecules: science, technology and applications. *New J. Phys.* **2009**, *11*, 055049.
- (7) Krens, R.; Friedrich, B.; Stwalley, W. C. *Cold Molecules: Theory, Experiment, Applications*; CRC Press, 2009.
- (8) Tarbutt, M. R. *Laser Cooling of Molecules*; Taylor & Francis, 2018.
- (9) Baum, L.; Vilas, N. B.; Hallas, C.; Augenbraun, B. L.; Raval, S.; Mitra, D.; Doyle, J. M. 1d magneto-optical trap of polyatomic molecules. *Phys. Rev. Lett.* **2020**, *124*, 133201.
- (10) Chin, C.; Flambaum, V.; Kozlov, M. Ultracold molecules: new probes on the variation of fundamental constants. *New J. Phys.* **2009**, *11*, 055048.
- (11) Baron, J.; Campbell, W. C.; DeMille, D.; Doyle, J. M.; Gabrielse, G.; Gurevich, Y. V.; Hess, P. W.; Hutzler, N. R.; Kirilov, E.; Kozyryev, I.; et al. Order of magnitude smaller limit on the electric dipole moment of the electron. *Science* **2014**, *343*, 269–272.
- (12) Cairncross, W. B.; Gresh, D. N.; Grau, M.; Cossel, K. C.; Roussy, T. S.; Ni, Y.; Zhou, Y.; Ye, J.; Cornell, E. A. Precision measurement of the electron’s electric dipole moment using trapped molecular ions. *Phys. Rev. Lett.* **2017**, *119*, 153001.
- (13) Ospelkaus, S.; Ni, K.-K.; Wang, D.; De Miranda, M.; Neyenhuis, B.; Quémener, G.; Julienne, P.; Bohn, J.; Jin, D.; Ye, J. Quantum-state controlled chemical reactions of ultracold potassium-rubidium molecules. *Science* **2010**, *327*, 853–857.
- (14) Quémener, G.; Julienne, P. S. Ultracold molecules under control. *Chem. Rev.* **2012**, *112*, 4949–5011.
- (15) Bohn, J. L.; Rey, A. M.; Ye, J. Cold molecules: Progress in quantum engineering of chemistry and quantum matter. *Science* **2017**, *357*, 1002–1010.
- (16) DeMille, D. Quantum computation with trapped polar molecules. *Phys. Rev. Lett.* **2002**, *88*, 067901.
- (17) Baranov, M. A.; Dalmonte, M.; Pupillo, G.; Zoller, P. Condensed matter theory of dipolar quantum gases. *Chem. Rev.* **2012**, *112*, 5012–5061.
- (18) Zhelyazkova, V.; Cournol, A.; Wall, T. E.; Matsushima, A.; Hudson, J. J.; Hinds, E.; Tarbutt, M.; Sauer, B. Laser cooling and slowing of CaF molecules. *Phys. Rev. A* **2014**, *89*, 053416.
- (19) Anderegg, L.; Augenbraun, B. L.; Chae, E.; Hemmerling, B.; Hutzler, N. R.; Ravi, A.; Collopy, A.; Ye, J.; Ketterle, W.; Doyle, J. M. Radio frequency magneto-optical trapping of CaF with high density. *Phys. Rev. Lett.* **2017**, *119*, 103201.
- (20) Lim, J.; Almond, J.; Trigatzis, M.; Devlin, J.; Fitch, N.; Sauer, B.; Tarbutt, M.; Hinds, E. Laser cooled YbF molecules for measuring the electron’s electric dipole moment. *Phys. Rev. Lett.* **2018**, *120*, 123201.
- (21) McNally, R. L.; Kozyryev, I.; Vazquez-Carson, S.; Wenz, K.; Wang, T.; Zelevinsky, T. Optical cycling, radiative deflection and laser cooling of barium monohydride ($^{138}\text{Ba}^1\text{H}$). *New J. Phys.* **2020**, *22*, 083047.
- (22) Kozyryev, I.; Baum, L.; Matsuda, K.; Augenbraun, B. L.; Anderegg, L.; Sedlack, A. P.; Doyle, J. M. Sisyphus laser cooling of a polyatomic molecule. *Phys. Rev. Lett.* **2017**, *118*, 173201.
- (23) Zeppenfeld, M.; Englert, B. G.; Glöckner, R.; Prehn, A.; Mielenz, M.; Sommer, C.; van Buuren, L. D.; Motsch, M.; Rempe, G. Sisyphus cooling of electrically trapped polyatomic molecules. *Nature* **2012**, *491*, 570–573.
- (24) Monroe, C.; Meekhof, D. M.; King, B. E.; Itano, W. M.; Wineland, D. J. Demonstration of a fundamental quantum logic gate. *Phys. Rev. Lett.* **1995**, *75*, 4714–4717.
- (25) Troiani, F.; Affronte, M. Molecular spins for quantum information technologies. *Chem. Soc. Rev.* **2011**, *40*, 3119–3129.
- (26) Park, J. W.; Yan, Z. Z.; Loh, H.; Will, S. A.; Zwierlein, M. W. Second-scale nuclear spin coherence time of trapped ultracold $^{23}\text{Na}^{40}\text{K}$ molecules. *Science* **2017**, *357*, 372–375.
- (27) Hudson, E. R.; Campbell, W. C. Dipolar quantum logic for freely rotating trapped molecular ions. *Phys. Rev. A* **2018**, *98*, 040302.
- (28) Rugango, R.; Goeders, J. E.; Dixon, T. H.; Gray, J. M.; Khanyile, N.; Shu, G.; Clark, R. J.; Brown, K. R. Sympathetic cooling of molecular ion motion to the ground state. *New J. Phys.* **2015**, *17*, 035009.
- (29) Bruzewicz, C. D.; Chiaverini, J.; McConnell, R.; Sage, J. M. Trapped-ion quantum computing: Progress and challenges. *Appl. Phys. Rev.* **2019**, *6*, 021314.
- (30) Schuster, D.; Bishop, L. S.; Chuang, I.; DeMille, D.; Schoelkopf, R. Cavity qed in a molecular ion trap. *Phys. Rev. A* **2011**, *83*, 012311.
- (31) Sinhal, M.; Willitsch, S. “Molecular-ion quantum technologies”. **2022**, arXiv:2204.08814, submitted 04-19-2022, accessed 03-13-2023.
- (32) Moreno-Pineda, E.; Godfrin, C.; Balestro, F.; Wernsdorfer, W.; Ruben, M. Molecular spin for quantum algorithms. *Chem. Soc. Rev.* **2018**, *47*, 501–513.
- (33) Albert, V. V.; Covey, J. P.; Preskill, J. Robust encoding of a qubit in a molecule. *Phys. Rev. X* **2020**, *10*, 031050.
- (34) Wakelam, V.; Herbst, E.; Loison, J.-C.; Smith, I.; Chandrasekaran, V.; Pavone, B.; Adams, N.; Bacchus-Montabonel, M.-C.; Bergeat, A.; Béroff, K.; et al. A kinetic database for astrochemistry (KIDA). *Astrophys. J., Suppl. Ser.* **2012**, *199*, 21.
- (35) McElroy, D.; Walsh, C.; Markwick, A.; Cordiner, M.; Smith, K.; Millar, T. The UMIST database for astrochemistry 2012. *Astron. Astrophys.* **2013**, *550*, A36.
- (36) O’Connor, A.; Urbain, X.; Stützel, J.; Miller, K.; Ruetter, N. d.; Garrido, M.; Savin, D. W. Reaction Studies of Neutral Atomic C with H_3^+ using a Merged-Beams Apparatus. *Astrophys. J., Suppl. Ser.* **2015**, *219*, 6.
- (37) De Ruetter, N.; Miller, K.; O’Connor, A.; Urbain, X.; Buzard, C.; Vissapragada, S.; Savin, D. W. Merged-beams reaction studies of O^+ . *Astrophys. J.* **2015**, *816*, 31.
- (38) Tran, T. D.; Rednyk, S.; Kovalenko, A.; Roučka, Š.; Dohnal, P.; Plašil, R.; Gerlich, D.; Glosík, J. Formation of H_2O^+ and H_3O^+ cations in reactions of OH^+ and H_2O^+ with H_2 : Experimental studies of the reaction rate coefficients from $T = 15$ to 300 K. *Astrophys. J.* **2018**, *854*, 25.
- (39) Hillenbrand, P.-M.; Bowen, K.; Liévin, J.; Urbain, X.; Savin, D. W. Experimental and Theoretical Studies of the Isotope Exchange Reaction $\text{H}_3^+ \rightarrow \text{H}_2^+$. *Astrophys. J.* **2019**, *877*, 38.

- (40) Kumar, S. S.; Grussie, F.; Suleimanov, Y. V.; Guo, H.; Kreckel, H. Low temperature rates for key steps of interstellar gas-phase water formation. *Sci. Adv.* **2018**, *4*, No. eaar3417.
- (41) Ryjkov, V. L.; Zhao, X.; Schuessler, H. A. Sympathetic cooling of fullerene ions by laser-cooled Mg^+ ions in a linear rf trap. *Phys. Rev. A* **2006**, *74*, 023401.
- (42) Hudson, E. R. Sympathetic cooling of molecular ions with ultracold atoms. *EPJ Tech. Instrum.* **2016**, *3*, 8.
- (43) Ladd, T. D.; Jelezko, F.; Laflamme, R.; Nakamura, Y.; Monroe, C.; O'Brien, J. L. Quantum computers. *Nature* **2010**, *464*, 45–53.
- (44) Nguyen, J. H.; Viteri, C. R.; Hohenstein, E. G.; Sherrill, C. D.; Brown, K. R.; Odom, B. Challenges of laser-cooling molecular ions. *New J. Phys.* **2011**, *13*, 063023.
- (45) Kang, S.-Y.; Kuang, F.-G.; Jiang, G.; Li, D.-B.; Luo, Y.; Feng-Hui, P.; Li-Ping, W.; Hu, W.-Q.; Shao, Y.-C. Ab initio study of laser cooling of AlF^+ and AlCl^+ molecular ions. *J. Phys. B: At., Mol. Opt. Phys.* **2017**, *50*, 105103.
- (46) Li, R.; Yuan, X.; Liang, G.; Wu, Y.; Wang, J.; Yan, B. Laser cooling of the SiO^+ molecular ion: A theoretical contribution. *Chem. Phys.* **2019**, *525*, 110412.
- (47) Chmaisani, W.; Elmoussaoui, S. Theoretical study of laser cooling of the tlf^+ molecular ion. *Phys. Chem. Chem. Phys.* **2021**, *23*, 1718–1726.
- (48) Karl, R.; Yin, Y.; Willitsch, S. Laser cooling of trapped ions in strongly inhomogeneous magnetic fields. *Mol. Phys.* **2023**, 2199099.
- (49) van Dishoeck, E. F.; Kristensen, L. E.; Mottram, J. C.; Benz, A. O.; Bergin, E. A.; Caselli, P.; Herpin, F.; Hogerheijde, M. R.; Johnstone, D.; Liseau, R.; et al. Water in star-forming regions: physics and chemistry from clouds to disks as probed by herchel spectroscopy. *Astron. Astrophys.* **2021**, *648*, A24.
- (50) Neufeld, D. A.; Wolfire, M. G. The cosmic-ray ionization rate in the galactic disk, as determined from observations of molecular ions. *Astrophys. J.* **2017**, *845*, 163.
- (51) Hodges, J. N.; Bernath, P. F. Fourier transform spectroscopy of the transition of OH^+ . *Astrophys. J.* **2017**, *840*, 81.
- (52) Gómez-Carrasco, S.; Godard, B.; Lique, F.; Bulut, N.; Klos, J.; Roncero, O.; Aguado, A.; Aoiz, F. J.; Castillo, J. F.; Goicoechea, J. R.; et al. OH^+ in astrophysical media: State-to-state formation rates, einstein coefficients and inelastic collision rates with He. *Astrophys. J.* **2014**, *794*, 33.
- (53) This branching ratio is observed between the states $A^3\Pi\ 0, 1$ and $X^3\Sigma^- 0, 0, 1$.
- (54) Vilas, N. B.; Hallas, C.; Anderegg, L.; Robichaud, P.; Winnicki, A.; Mitra, D.; Doyle, J. M. Magneto-optical trapping and sub-doppler cooling of a polyatomic molecule. *Nature* **2022**, *606*, 70–74.
- (55) Emsley, J. *The Elements: Oxford Chemistry Guides*; Oxford University Press, 1995.
- (56) Shuman, E.; Barry, J.; Glenn, D.; DeMille, D. Radiative force from optical cycling on a diatomic molecule. *Phys. Rev. Lett.* **2009**, *103*, 223001.
- (57) March, R. E. Quadrupole ion traps. *Mass Spectrom. Rev.* **2009**, *28*, 961–989.
- (58) Yurchenko, S. N.; Szabó, I.; Pyatenko, E.; Tennyson, J. line lists : spectroscopy of lowest eight electronic states of C_2 . *Mon. Not. R. Astron. Soc.* **2018**, *480*, 3397–3411.
- (59) Bernath, P. F. Mollist: molecular line lists, intensities and spectra. *J. Quant. Spectrosc. Radiat. Transfer* **2020**, *240*, 106687.
- (60) Hodges, J. N.; Bittner, D. M.; Bernath, P. F. Improved ultraviolet and infrared oscillator strengths for OH^+ . *Astrophys. J.* **2018**, *855*, 21.
- (61) Bigagli, N.; Savin, D. W.; Will, S. Laser cooling scheme for the carbon dimer ($^{12}\text{C}_2$). *Phys. Rev. A* **2022**, *105*, L051301.
- (62) Merer, A.; Malm, D.; Martin, R.; Horani, M.; Rostas, J. The ultraviolet emission spectra of OH^+ and OD^+ . rotational structure and perturbations in the $A^3\Pi-X^3\Sigma^-$ transition. *Can. J. Phys.* **1975**, *53*, 251–283.
- (63) Bernath, P. F. *Spectra of Atoms and Molecules*; Oxford University Press, 2020.
- (64) Sun, Q.; Dickerson, C. E.; Dai, J.; Pope, I. M.; Cheng, L.; Neuhauser, D.; Alexandrova, A. N.; Mitra, D.; Zelevinsky, T. “Probing the limits of optical cycling in a predissociative diatomic molecule”. **2023**, arXiv:2306.01184, submitted 06-01-2023, accessed 06-19-2023.
- (65) Rosa, M. D. Laser-cooling molecules. *Eur. Phys. J. D* **2004**, *31*, 395–402.
- (66) Tarbutt, M.; Sauer, B.; Hudson, J.; Hinds, E. Design for a fountain of YbF molecules to measure the electron's electric dipole moment. *New J. Phys.* **2013**, *15*, 053034.
- (67) Fitch, N.; Tarbutt, M. Chapter Three—Laser-Cooled Molecules”. *Advances in Atomic, Molecular, and Optical Physics*; Academic Press, 2021; Vol. 70, pp 157–262.
- (68) Corato-Zanarella, M.; Gil-Molina, A.; Ji, X.; Shin, M. C.; Mohanty, A.; Lipson, M. Widely tunable and narrow-linewidth chip-scale lasers from near-ultraviolet to near-infrared wavelengths. *Nat. Photon.* **2023**, *17*, 157–164.